Journal of Hydrology 580 (2020) 124321

Contents lists available at ScienceDirect

Journal of Hydrology

journal homepage: www.elsevier.com/locate/jhydrol

Research papers

Sensitivity of using stable water isotopic tracers to study the hydrology of isolated wetlands in North Florida

Glynnis C. Bugna[a], Johnny M. Grace[b], Yuch-Ping Hsieh[a,*]

[a] Center for Water Resources, College of Agriculture and Food Sciences, Florida A&M University, Tallahassee, FL 32307, USA
[b] USDA Forest Service, Southern Research Station, Center for Forests and Watershed Health, Tallahassee, FL 32307, USA

ARTICLE INFO

This manuscript was handled by Marco Borga, Editor-in-Chief, with the assistance of Daniele Penna, Associate Editor

Keywords:
Isolated wetlands
Oxygen and hydrogen tracers
Hydrology

ABSTRACT

Hydrology of forested wetlands is critical to the ecosystem functions and services of the forests. Our understanding of the hydrology of those wetlands, however, is very limited most likely due to the tediousness and costs of monitoring those scattered small wetlands by the traditional methods. Stable isotope ratios of oxygen ($\delta^{18}O$) and hydrogen ($\delta^{2}H$) in water may provide us a much simpler alternative to study the hydrology of those wetlands. We investigated the sensitivity and resolution of using natural stable water isotopes to quantify the hydrology of those isolated wetlands in the forests of North Florida. The observed Local Meteoric Water Line (LMWL) [$\delta^{2}H = 7.7*\delta^{18}O + 9.2$ ($r^2 = 0.97$, $n = 202$)] followed closely to the Global Meteoric Water Line (GMWL), indicating the local rains were formed following a general isotopic equilibrium condition. Using data collected between 2014 and 2017, we observed a negative linear correlation between monthly total rain and the weight of its isotopic signature. There was no significant effect of temperature or humidity on the isotopic signatures of the rains. The water isotopes of the ephemeral ponds and sinks, on the other hand, were significantly enriched relative to the precipitation. The local evaporation lines (LEL) of the studied ephemeral ponds and sinks indicated significant evaporation. The isotope data indicated that the ephemeral Pond 55 and Pond 12 were rain fed while the water source to Blue Sink was a mixture of precipitation and groundwater. We showed that the significant differences in stable water isotopic signatures among the precipitation (especially during tropical storms and hurricanes), surface water and ground water can be used to trace the hydrological budgets and processes of forested wetlands in North Florida.

1. Introduction

The stable oxygen and hydrogen isotopes have been used extensively as conservative tracers in hydrological studies (Gremillion and Wanielista, 2000). For example, they have been used to determine the sources of waters, flow patterns, and mixing of waters in different bodies of water (e.g., Katz and Bullen, 1996; Araguás-Araguás et al., 2000; Gremillion and Wanielista, 2000). Furthermore, through changes of its isotope composition within the water cycle, the water can be related to the different phases of the cycle (Gat, 1996). Isotope have also been used as tracers to reconstruct continental paleoclimatology and paleohydrology (e.g., Rozanski et al., 1992; Koch et al., 1995; Seal and Shanks, 1998; Baczynski et al., 2017).

On a global scale, the average relationship between oxygen ($\delta^{18}O$) and hydrogen ($\delta^{2}H$) isotopic ratios in natural meteoric waters show a distinct empirical relationship that can be summed up by the following Global Meteoric Water Line or GMWL (Craig, 1961): $\delta^{2}H = 8*\delta^{18}O + 10$. Local precipitation data give rise to their own $\delta^{18}O$-$\delta^{2}H$ relationship which is the Local Meteoric Water Line or LMWL. Any deviation (e.g., moisture re-cycling, source water evaporation), or the lack there of, between the LMWL and the GMWL helps to understand the precipitation pathways of a given region (Breitenbach et al., 2010). The same is true with the comparison between LMWL and the local evaporation line (LEL, $\delta^{18}O$-$\delta^{2}H$ relationship) of natural surface waters. Lower LEL slopes, typically 5–6, refer to enrichment due to evaporation of the waters (e.g., Gibson et al., 2008; Dogramaci et al., 2012).

Ephemeral ponds are isolated and seasonal wetland systems, i.e. depressions that remain inundated for extended periods during a given year but may dry out completely (Means, 2008). They occur in most regions throughout the world and are often found in the southeastern US Coastal Plain (Tiner, 2003; Zedler, 2003; Brooks, 2009). The dynamics of ephemeral wetlands, and their counterparts in various regions (e.g., prairie potholes, playas, vernal pools), have received some attention in previous research but remains poorly understood (Zedler,

* Corresponding author.
E-mail address: yuch.hsieh@famu.edu (Y.-P. Hsieh).

https://doi.org/10.1016/j.jhydrol.2019.124321
Received 9 April 2019; Received in revised form 31 October 2019; Accepted 5 November 2019
Available online 11 November 2019

2003; Bauder, 2005; Brooks, 2009; Roznik et al., 2009). It is recognized that these ephemeral systems, particularly their water flow connectivity and ecology, are as variable as their spatial distribution (Zedler, 2003; Brooks, 2009). The water balances on these systems are likely highly variable over time due to the influence of evapotranspiration (ET) and groundwater exchange (Hayashi and Rosenberry, 2002) in smaller scale forested ecosystems. Ephemeral wetlands like the prairie pothole wetlands likely shift from groundwater-fed systems to primarily precipitation-(and surface runoff-) fed systems during most of growing season (Winter and Rosenberry, 1998).

The hydrology of ephemeral wetlands has not been well described and their reliance on surface and subsurface water charging/discharging requires further study especially in humid subtropical regions like the Florida Coastal Plain region. The influence of climate and the interaction between surface and subsurface sources and sinks on the ephemeral wetland hydroperiod (period of inundation) is of particular interest in this region. There are still major gaps in the understanding related to the hydrological, ecological and herpetological benefits (services) of these systems (e.g., Means, 2008; Greenberg et al., 2015; Chandler et al., 2016; Chandler et al., 2017; Means et al., 2017; Zhu et al., 2017). Our poor understanding of the hydrological budgets and processes in those isolated wetlands is most likely due to the tediousness and costly traditional monitoring methods. Isotopic tracer method, however, may provide a much simpler alternative for the study of hydrology in those wetlands. With this in mind, the primary goal of this research was to determine the sensitivity and resolution of the stable water isotopes as hydrological tracers for isolated forested wetlands in the region. Our hypothesis is that oxygen and hydrogen isotopes are sensitive tracers for quantifying hydrologic budget and processes of isolated wetlands in Florida, especially during hurricane and tropical storm situations. Here we present the isotopic data of precipitations, surface water, and soil pore water of the selected isolated wetlands in the Apalachicola National Forest (ANF) and determined the significance and the optimal situations when those isotopic signals can be used to quantify the hydrologic processes of those wetlands.

2. Experimental

2.1. Lake Munson Sandhills (LMS) geology

The study sites (Pond 55, Pond 12 and Blue Sink; Fig. 1) are located within the Leon County (FL) LMS region at the western edge of the Woodville Karst Plain (WKP; Hendry and Sproul, 1966). Pond 55 and Pond 12 are among at least 200 similar isolated forested wetland ponds in the ANF (Means et al., 2017). According to the National Wetland Inventory (https://www.fws.gov/wetlands/data/mapper.html), Pond 55 and Pond 12 are classified as palustrine systems dominated by persistent herbaceous vegetation with a water regime that is semi-permanently flooded. Blue Sink, on the other hand, is classified as a palustrine system with at least 25% cover of particles smaller than 6–7 cm, a vegetative cover less than 30% and a permanently flooded water regime (National Wetlands Inventory, accessed 27-Oct-2019). These three sites has been chosen for their natural condition and accessibility.

The WKP is characterized by a thin veneer of unconsolidated and undifferentiated Pleistocene quartz sands and shell beds, overlying Oligocene and Miocene age limestones (Hendry and Sproul, 1966; Rupert, 1988; Katz, 2001; Kincaid and Werner, 2008). Porous and permeable veneering sands allow rainwater to rapidly move into the underlying limestone strata that make up the Upper Floridan Aquifer (UFA). Groundwaters from the UFA is the source of water supply for the nearest city Tallahassee, and for parts of the surrounding areas (Davis, 1996). The underlying limestones are very soluble and have undergone considerable solution by the action of these percolating groundwaters. As a result, the area has been continuously and rapidly lowered from original level, and is presently covered with sinks that appear as shallow sand-filled depressions (Hendry and Sproul, 1966; Katz, 2001).

The LMS region of the Apalachicola National Forest near Tallahassee, FL is specifically dotted with by numerous shallow depressions that represent karst features at depth mantled by overlying sands, silts and clays (Hendry and Sproul, 1966). While the WKP allows for a rapid groundwater recharge, the silts and clays of the adjoining Apalachicola Coastal Lowlands interfinger with the sands of the LMS region, resulting in poorer permeability, more restricted downward percolation of the groundwater, less solution of the limestone bedrock, and therefore, minimal change from the original depositional surface and elevation of the WKP (Hendry and Sproul, 1966).

Many of the shallow depressions in the LMS region are seasonally filled with water during the rainy season and gradually drain out during periods of low rainfall (Means, 2008). They host a rich variety of plant, animal and insect species that depend on the cyclical filling and draining of the ephemeral wetlands for at least part of their life cycles (Means, 2008). Soil surrounding the area is moderately drained and rapidly permeable Ortega (thermic, uncoated Typic Quartzipsamments) sands with 0 to 5 percent slopes (Soil Survey of Leon County, Florida, 1981). The sandhills region is characteristic of the southeastern US Coastal Plain ecoregion and was historically dominated by fire-dependent longleaf pine (*Pinus palustris*) communities (Johnson and Gjerstad, 2006).

2.2. Meteorological data

Online meteorological data (temperature, relative humidity and rainfall amount) from Sail High Weatherstem Station, Tallahassee, FL (https://leon.weatherstem.com/) was used as a data source since it is one of the nearest weather stations with data dating back to at least 2014. The station is located within a 10-km radius from the study sites. During the sampling period, three named storms passed through the area: tropical storm Colin and Category 1 hurricane Hermine in 2016, both of which caused direct impacts, and tropical storm Cindy in 2017, which contributed heavy rainfall to the Leon County area. According to the Köppen climate classification, north Florida's humid subtropical climate is characterized by hot and humid summers and mild to chilly winters (Peel et al., 2007). The colder months are normally from December to February, while the hotter months are from May to September. Daily mean temperatures in 2015–2017 ranged from below freezing to 24 °C during the winter season, and between 16 and 31 °C during the summer season. Mean monthly summer temperatures (24–29 °C) were generally 10–15 °C higher than in winter (~14 °C, Fig. 2a). During the 3-year sampling period, mean monthly humidity values ranged between 71 and 82% (Fig. 2b). The meteorological data also showed higher total rainfall amounts during the summer (Fig. 2c), and lower amounts during the fall and spring months, generally following the trend of normal monthly rainfall amounts for Tallahassee, FL (https://climatecenter.fsu.edu/products-services/data/1981–2010-normals/tallahassee). Based on the online data, 8.9%, 27.1% and 64% of the 1,204 study period days could be classified as heavy rain (experiencing > 30 mm/hr rain intensities), light/medium rain (< 30 mm/hr intensities) and dry days, respectively. The heavy rain days while few, accounted for 69.5% of the total recorded precipitation (~3780 mm rain).

2.3. Water sampling

Samples from more than 126 rain events were collected from November 2014 to August 2017 at the Florida A&M University (FAMU) campus, the Tallahassee International Airport and the northeastern (NE) part of Tallahassee, FL. Rainwater samples were also collected at Pond 55 (Fig. 1) from April 2015 to May 2017, and at Pond 12 (Fig. 1) from April 2015 to November 2015, respectively.

Water samples were collected using rain collectors consisting of a high density polyethylene (HDPE) bottle with a funnel placed on top.

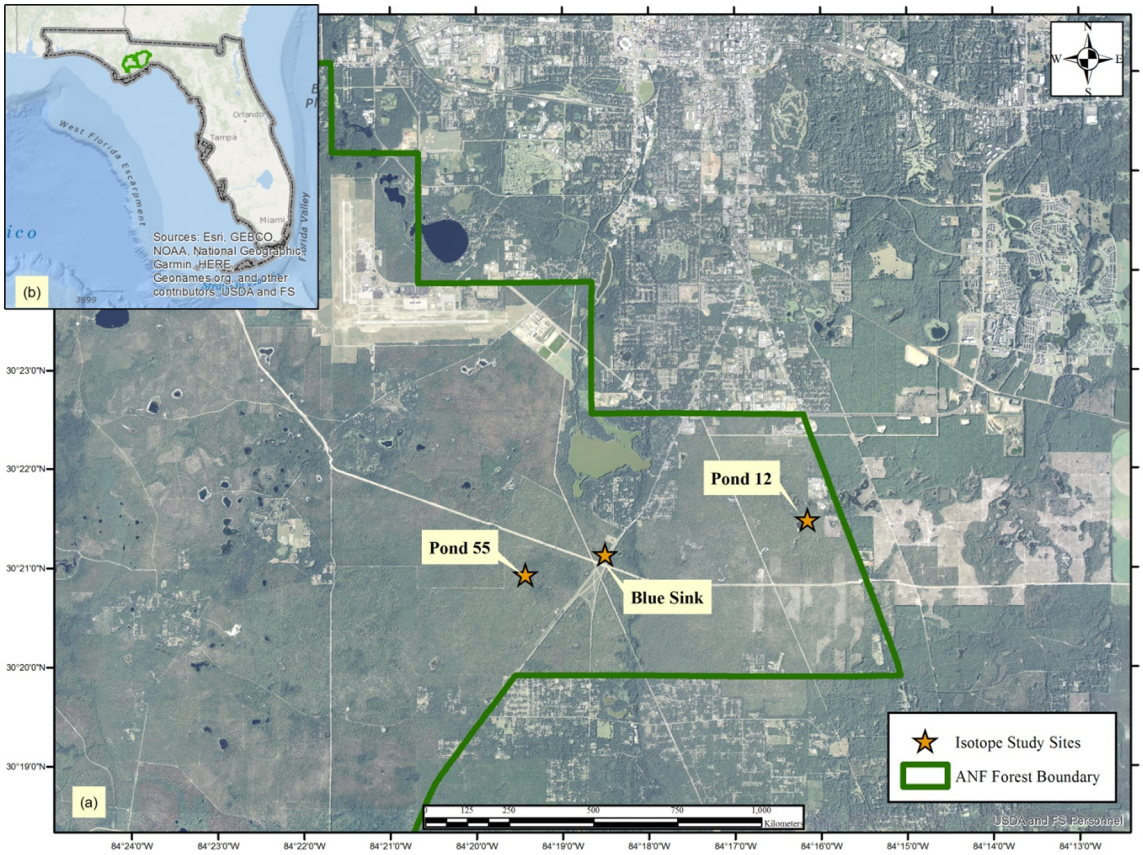

Fig. 1. Locations of the study sites within the Apalachicola National Forest (with green boundary) south of Tallahassee, FL, USA.

These rain collectors were placed under a forest canopy at Pond 55, under a less dense canopy at Pond 12 and under no cover at the FAMU campus. Immediately after each event, collected rain water samples were transferred to 60-mL HDPE bottles, tightly capped and stored in a refrigerator prior to isotopic analysis. Samples were only collected during days when it was forecasted to rain at least 0.1″ (2.54 mm). Previous studies had shown that rainwater samples typically have d-excess values greater than 0 so that any value below 0 is indicative of evaporation in the rain collectors or sampling containers (Welker, 2000; Harvey, 2001; Gammons et al., 2006; Sjostrom and Welker, 2009).

In addition to the rainwater samples, surface and soil pore water samples were also collected. Temporal surface waters were collected from Pond 55, Pond 12 and Blue Sink (Fig. 1), depending on the forecasted rain. We aimed to conduct the samplings so that we collected surface water samples before and right after a significant rain event. Surface waters were sampled by hand by first rinsing a 60-mL HDPE bottle with the water twice before collection. Bottles were filled to the brim, tightly capped and transported to the laboratory and stored in the refrigerator prior to analysis. To simulate the evaporation and contribution of rainwaters, closed bottom/open top PVC cylinders [38–54 (H) × 15 cm (D)] were installed at Pond 55 and Pond 12. At each site, the PVC cylinder contained 8 L (Pond 55) and 5 L (Pond 12) of their respective surface waters. Both also contained Onset HOBO water loggers (Onset Computer Corporation, Bourne, MA) that recorded data at 10-min intervals. Water samples from the PVC experiments were collected almost at the same time as the pond water samples. PVC water volume collected for each sampling was only 7 mL so it was a very small fraction relative to the total volume even with evaporation (< 0.2%). Collected PVC water samples were stored cold in 7-mL shell vials with closures (Kimble part number 60965D-1). The integrity of the vial-stored sample with regards to evaporation was tested on triplicate tap water volumes (1, 3, 5 mL) in the 7-mL shell vials, which showed negligible evaporation effect (0.01–0.02% CV) based on weight in a 77-hr storage experiment. With the PVC, the only water input and output are rain and evaporation, respectively, while for the pond, they could be rain (input), evaporation (output) and something else (overland flow, shallow groundwater, etc.). The similarity between the pond and PVC LELs would indicate that rainfall and evaporation are the dominant input and output, respectively.

Soil pore water samples were collected at the upland forest near Pond 55, when ground water table was higher than the surface water of the pond. Soil cores below the groundwater table interface were taken using soil augers. In the laboratory, porewater was collected immediately as free water that separated from the water-saturated soil cores. We used 1-mL plastic transfer pipets with bulbs for transferring porewater into shell vials or HDPE bottles. These samples were processed similarly to the other water samples for isotope analysis. A total of nine (9) soil pore water samples were taken from samplings conducted in April 2015 (3 samples), August 2016 (3) and February 2017 (3).

2.4. Isotope analysis

Water samples were prepared for isotope analysis by withdrawing a 5–10 mL aliquot using a syringe. With a 0.45 µm filter attached to the tip, approximately 1 mL of the filtered sample was poured directly into a 2-mL auto-injector vial and closed with a septum cap. Samples were analyzed for $\delta^{18}O$ and $\delta^{2}H$ using a Liquid Water Isotope Analyzer (LWIA)-generation 2 (ABB – Los Gatos Research, San Jose, CA) with an attached auto-injector for analysis. The LWIA-gen2 uses off-axis integrated cavity output spectroscopy (OA-ICOS) to analyze the water isotopes (e.g., Baer et al., 2002; Sturm and Knohl, 2010). Briefly, the method measures the mixing ratios of three water isotopologues

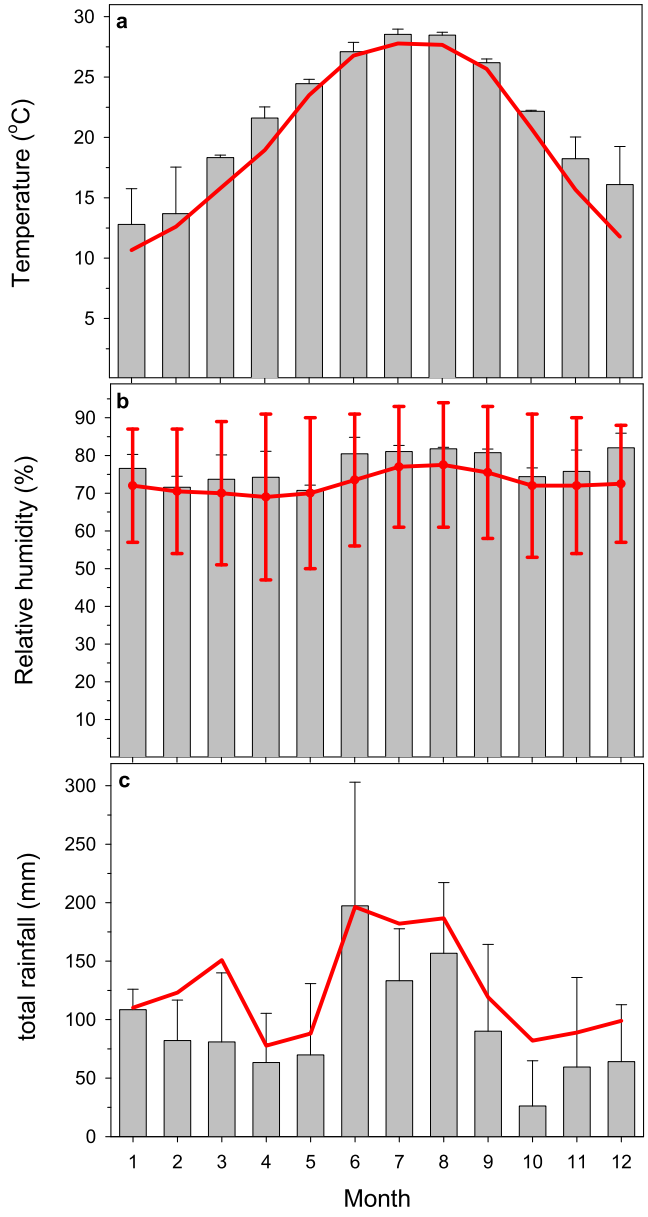

Fig. 2. Meteorological data (2015–2017) collected from a nearby weather station. The solid lines represent normal average monthly temperatures, relative humidity values and rainfall amounts for Tallahassee, FL. Data taken from online databases.

$^{1}H^{16}O^{1}H$, $^{1}H^{18}O^{1}H$ and $^{2}H^{16}O^{1}H$ by scanning over three nearby absorption lines with similar line strengths and wavelength. The beam of an infrared diode laser is directed off-axis into an optical cavity, resulting in an effective optical path length in the order of several kilometers and higher absorption signals (Sturm and Knohl, 2010). Manufacturer-supplied certified standard solutions (with known $\delta^{18}O$ and $\delta^{2}H$ values) were run after each set of five samples. Every vial containing either standard or sample was analyzed six times with means and standard deviations taken from the last four replicates. This was done in order to eliminate carryover effects from the previous sample. Results were expressed in δ notation relative to Vienna Standard Mean Ocean Water (VSMOW):

$$\delta\ (‰) = \left(\frac{R_{sample}}{R_{standard}} - 1\right) \times 1000 \quad (1)$$

where R = $^{18}O/^{16}O$ or $^{2}H/^{1}H$. The more the negative the δ value, the more depleted in either ^{18}O or ^{2}H. The repeated measures error (SD) of this method is < 0.3‰ and < 2‰ for $\delta^{18}O$ and $\delta^{2}H$, respectively. The OA-ICOS method had been verified with the isotope ratio mass spectrometer method with very good comparability between the two (e.g., Lis et al., 2008; Penna et al., 2010; Berman et al., 2013).

2.5. Evaporation experiments

We also conducted a 14-day laboratory evaporation experiment using Pond 55 natural surface waters. Glass beakers (250-mL) were initially added with 200 g of water sample by weighing. Beakers were then left outside during the day to evaporate, but were brought inside at the end of each day or when it rained. At the end of each of day, beakers were weighed, subsampled (one 7-mL sample per beaker), and weighed again. Measured accumulated evaporative water loss was calculated as the difference in weight between the measured weight (at that time point) and the initial weight (at the start of the experiment), taking into account the amount of the subsample removed. We assumed that the water density was 0.998 g/mL at 22 °C. An overall cumulative water loss was calculated at the end of the experiment, and the $\delta^{18}O$ and $\delta^{2}H$ values of all samples were determined.

2.6. Statistical treatment

For the statistical treatment of data, we utilized the IBM SPSS (Statistical Package for the Social Sciences) software (Armonk, NY) for performing comparison of means (one way ANOVA) as related to temperature, humidity, rain amount and seasonality, while correlations between parameters were analyzed using Pearson's correlation (one-tailed) at the 95% confidence level.

3. Results and discussion

3.1. Isotopic composition of precipitation

Collected rainwater samples exhibited a range of $\delta^{18}O$ (−14.7‰ to +1.0‰) and $\delta^{2}H$ values (−108‰ to +11.5‰) (Table 1). Rain samples with the most depleted isotope signals observed were associated with tropical storms and hurricanes that passed through the area. Water isotopes depleted to the narrow ranges of –14.3 to –14.7‰ ($\delta^{18}O$) and −107.3 to −107.8‰ ($\delta^{2}H$) during the hurricane Hermine and tropical storm Colin events, which dropped at least 102 mm of rain each in the area. This is similar to a number of studies that also showed more depleted $\delta^{18}O$ signals from tropical storms and hurricanes (e.g., Gedzelman and Lawrence, 1982; Gedzelman and Lawrence, 1990; Lawrence, 1998; Lawrence et al., 2002; Good et al., 2014; Lane et al., 2017; Vieten et al., 2018). Lawrence et al. (1998) noted that the low isotope ratios of rains in hurricanes is a consequence of their longevity, size and high precipitation efficiency, defined as the fraction of vapor

Table 1
Oxygen and hydrogen isotopic ratios of rain collected during 2014–2017. Numbers enclosed in parentheses denote standard deviations.

Rain	Statistic	$\delta^{18}O$ (‰)	$\delta^{2}H$ (‰)	d-excess
All rain	range	−14.7 to 1.0	−107.8 to 11.5	0.6 to 22.7
	weighted mean	−5.1	−30.2	10.4
	n	202	202	202
tropical storm Colin	mean	−12.5 (1.9)	−92.9 (14.7)	6.8 (0.1)
(June 2016)	n	2	2	2
hurricane Hermine	mean	−10.2 (3.0)	−72.4 (24.7)	9.1 (4.2)
(Cat. 1, Sep. 2016)	n	7	7	7
tropical storm Cindy		−4.9	−25.3	13.7
(June 2017)	n	1	1	1

that condenses and reaches the ground as precipitation. The higher the precipitation efficiency, the closer the rain $\delta^{18}O$ approaches the more depleted $\delta^{18}O$ of the source vapor. For instance, Lawrence and Gedzelman (1996) showed a 93% precipitation efficiency for tropical storms with a $\delta^{18}O$ signature of −9.3‰ when compared to a mean source vapor $\delta^{18}O$ signature of −12.2‰.

The source of precipitation to the study area may change seasonally, with convection style thunderstorms delivering rainfall during the summer months and with fall, winter and spring rains being associated with frontal systems that are driven west to east by jet streams (Lambert and Aharon, 2010). Sjostrom and Welker (2009) observed that based on analysis of air mass back-trajectory models, central Florida (e.g., Tampa) could have four possible sources of rainfall: Gulf, Mid Atlantic, Continental and Pacific. Gulf-sourced air masses are those that originated in the Caribbean Sea, Gulf of Mexico or in the Gulf Coast Region of the United States dominated during the spring and summer seasons (60–66% of total seasonal rain) while Continental- and Gulf-derived precipitation (50% and 40%, respectively) dominated during the winter season. Continental-derived air masses are such that originated and remained in the interior of the higher latitudes of North America without interacting with major western mountain ranges (Sjostrom and Welker, 2009). In general, rain sources originating from high latitude area tended to be have more depleted $\delta^{18}O$ and $\delta^{2}H$ values, and higher d-excess values. It has been reported that precipitation with d-excess values greater than 15 strongly suggests input from Continental sources (Harvey, 2001; Sjostrom and Welker, 2009). In this study, we did not observe a statistically significantly seasonality in isotope values ($p < 0.05$; Table 2, Fig. 3) except during the hurricane season when hurricanes and tropical storms contribute much depleted isotopic signals (Fig. 3, as shown by the slash-marked vertical bars). Data containing d-excess values > 15 represented only 13.4% of the total rainfall days, which could imply a predominant Gulf of Mexico rain source throughout the year. The lack of seasonality is also more expected in low latitudes like Florida than those in mid or high latitudes (Dansgaard, 1964; Fricke and O'Neil, 1999; Sjostrom and Welker, 2009).

No significant differences in isotopic signatures were observed among rains collected among Pond 55, Pond 12 and FAMU campus (Table 3), indicating not only a similar rain source but also an insignificant canopy effect ($p < 0.05$). The non-location effect was expected because the three sampling sites are within a 10-km radius while the lack of canopy effect was most likely due to the fact that longleaf pine ecosystems generally consist of sparse to open canopies (Oswalt et al., 2012). The rain $\delta^{18}O$ and $\delta^{2}H$ values from the three sites in Tallahassee showed minimal evaporation based on the LMWLs (Table 3). The LMWL from NE Tallahassee area in particular showed no rainfall evaporation since most of the samples were taken during passage of a tropical storm. Concern had been warranted when we removed rainfall $\delta^{18}O$ data with negative d-excess values, especially if these data were from sites with canopy cover (e.g., Allen et al., 2017; Gautam et al., 2017). The excluded data in this study represented only 1.9% (4 out of 206 data points) of the total data, with only one (1) data point (out of 46) removed from Pond 55 (with forest canopy, i.e., throughfall data) and three (3) data points from FAMU site (no canopy, i.e., rainfall data). We assumed that these outliers were due to post collection evaporation.

Table 2
Seasonal local meteoric water lines in Tallahassee, FL based on rainfall samples collected at the FAMU campus from 2014 to 2017. There is no significant difference among the four seasons ($p < 0.05$).

Season	Seasonal Local Meteoric Water Line (LMWL)	r^2	n
Winter (Dec–Feb)	$\delta^{2}H = 7.2*\delta^{18}O + 9.1$	0.94	19
Spring (Mar–Apr)	$\delta^{2}H = 7.1*\delta^{18}O + 6.7$	0.86	26
Summer (May–Sep)	$\delta^{2}H = 7.6*\delta^{18}O + 8.4$	0.97	74
Fall (Oct–Nov)	$\delta^{2}H = 7.3*\delta^{18}O + 6.2$	0.98	10

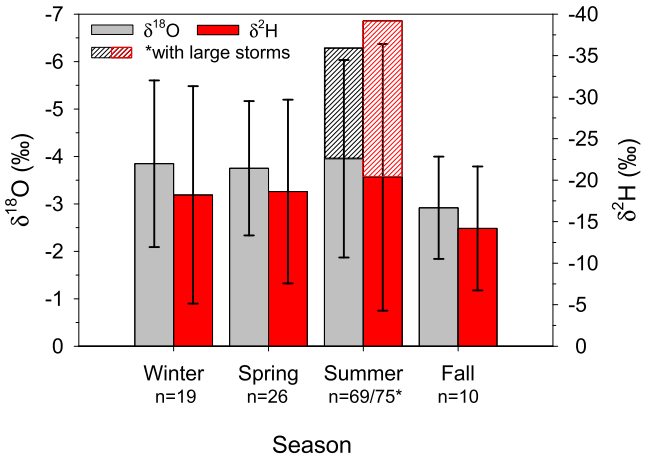

Fig. 3. Seasonal mean weighted $\delta^{18}O$ and $\delta^{2}H$ and their weighted standard deviations. There was lacking seasonality in the isotopic signatures except during the hurricane season when hurricanes and tropical storms contribute much depleted isotopic signals, as shown by the slash-marked vertical bars.

Table 3
Local meteoric water lines within Tallahassee, FL and the surrounding vicinities. Rainwater samples were collected from 2014 to 2017. There is no significant difference among the individual LMWLs ($p < 0.05$).

Vicinity	Local Meteoric Water Line (LMWL)	r^2	n
FAMU campus	$\delta^{2}H = 7.5*\delta^{18}O + 8.4$	0.96	127
Pond 55	$\delta^{2}H = 7.5*\delta^{18}O + 8.9$	0.95	46
Pond 12	$\delta^{2}H = 7.5*\delta^{18}O + 8.1$	0.96	16
NE Tallahassee	$\delta^{2}H = 8.3*\delta^{18}O + 13.6$	0.98	13

While the rainfall $\delta^{18}O$ values were similar to the throughfall values in this study, Xu et al. (2014) had shown that instead of values becoming more enriched due to evaporation, throughfall $\delta^{18}O$ values could also become more depleted.

Combining all rain isotope data, the Tallahassee LMWL of $\delta^{2}H = 7.7*\delta^{18}O + 9.2$ ($r^2 = 0.97$, n = 202) follows closely the Global Mean Water Line (GMWL, Fig. 4), indicating mostly isotopic equilibrium conditions during rain formation. The slight deviation from the GMWL suggests a minimal evaporation effect during rainfall of event-based samples. The weighted rain $\delta^{18}O$ and $\delta^{2}H$ signatures for the

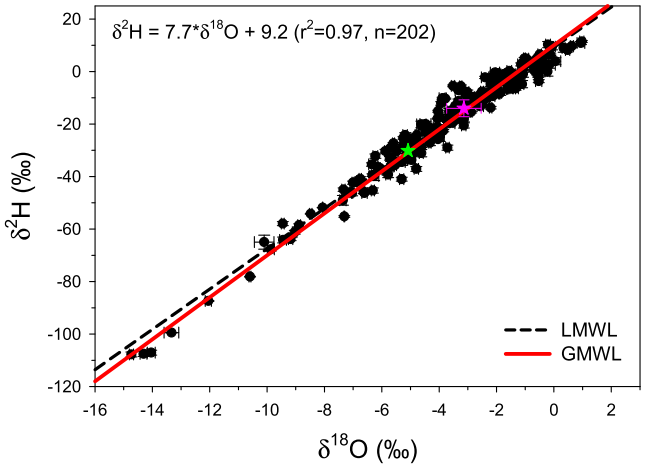

Fig. 4. The LMWL based on all Tallahassee precipitation data from 2014 to 2017. The LMWL is similar to the GMWL. The green star represents the mean weighted isotopic rain signature of all data ($\delta^{18}O = -5.1‰$, $\delta^{2}H = -30.2‰$). The pink star represents the mean pore water isotope signature ($\delta^{18}O = -3.1 \pm 0.6‰$, $\delta^{2}H = -14.0 \pm 3.2‰$, n = 9).

Table 4
Local Meteoric Water Lines derived from different humid, subtropical locations in Florida.

Location	LMWL	r^2	n	Reference
Tallahassee, FL (2006–2011)	$\delta^2H = 8.1*\delta^{18}O + 13.3$[a]	0.98	43	Odezulu (2011)
Pensacola, FL (2004–2010)	$\delta^2H = 6.8*\delta^{18}O + 9.6$[b]	0.86	250	Odezulu (2011)
Marianna, FL (2006–2007)	$\delta^2H = 5.8*\delta^{18}O + 4.1$[a]	0.99	13	Onac et al. (2008)
Ocala, FL (2006–2007)	$\delta^2H = 5.5*\delta^{18}O + 2.6$[a]	0.93	12	Onac et al. (2008)
South Lido/Tampa Bay, FL (1999–2001)	$\delta^2H = 7.6*\delta^{18}O + 10.0$[c]	0.99	128	Sjostrom and Welker (2009)
Tallahassee, FL (2014–2017)	$\delta^2H = 7.7*\delta^{18}O + 9.2$[b]	0.97	202	This study

[a] Derived from monthly weighted rain data.
[b] Derived from individual rain events.
[c] Derived from 24-hr weighted rain data.

entire data using online rainfall data are −5.1‰ and −30.2‰, respectively (green star, Fig. 4). Odezulu (2011) previously collected $\delta^{18}O$ and δ^2H data from monthly accumulated rainfall from 2006 to 2009 in Tallahassee that showed an LMWL of $\delta^2H = 8.1*\delta^{18}O + 13.3$ ($r^2 = 0.98$, n = 43; Table 4) similar to the GMWL. Wang et al. (2018) studied the influence of heavy and small precipitation on LMWLs by comparing event-based and monthly weighted LMWLs. Their study showed that the inclusion of rain isotope data from rainfalls > 1 mm showed a statistically significant larger LMWL slope for weighted data. However, if only isotope data from > 5 mm rains were used, there was no significant difference between weighted and unweighted data (Wang et al., 2018). In this study, we only collected samples from rains that were > 0.1″ (2.54 mm). The two Tallahassee LMWL data, taken at different sampling periods, may not be exactly the same but both did show similarity to the GMWL. Our data also agreed with data collected in South Lido and Tampa Bay, FL (Table 4; Sjostrom and Welker, 2009). However, at Central (Ocala) Florida and other North Florida (e.g., Marianna) sites having similar humid subtropical climate classifications, water isotopic data showed much lower LMWL slopes and hence significantly more evaporation of rains after they were formed despite similar time periods (Table 4). Odezulu (2011) suggested that closer proximity of Pensacola rainfall to its $\delta^{18}O$-enriched source (i.e., Gulf of Mexico) resulted in less isotope fractionation compared to those observed in a more inland location like Tallahassee.

Previous studies on tropical low latitude precipitation have reported that higher rainfall amounts were generally inversely correlated with isotopic signals known as the amount effect (Dansgaard, 1964; Lawrence et al., 1998; Coplen et al., 2000). In contrast, Permana et al. (2016) suggested that rather than amount, rain condensation mechanisms (e.g., atmospheric temperature in high reaching clouds; Otte et al., 2017) may have an equally if not greater influence on rainfall isotopic composition of tropical convective precipitation. The fractionation and exchange process that were related to the amount effect were particularly important at the beginning of the shower, or during a short shower before the air beneath the rain cloud becomes saturated and achieved isotopic equilibrium with the falling rain (Dansgaard, 1964; Hartley, 1981; Midwood et al., 1998). This leads to relatively enriched precipitation during periods of light rain and a more depleted signature with prolonged rainfall (Midwood et al., 1998; Dogramaci et al., 2012). A significant inverse correlation was observed in our study between $\delta^{18}O$ and rainfall amount ($p < 0.05$, Fig. 5) using monthly weighted values and rainfall totals using data from one site (i.e., FAMU campus). Similarly, we also found significant inverse correlation between rainfall amount and monthly weighted δ^2H ($p < 0.05$).

Our results showed that on average, the precipitation $\delta^{18}O$ and δ^2H became depleted by 1.95‰ and 14.8‰, respectively, for every 100 mm increased rainfall (Fig. 5). Lachniet and Patterson (2009) had suggested that the smaller $\delta^{18}O$ gradient (1.25‰/100 mm rainfall) in northern Central America and Mexico was due to a smaller rainout fraction of air masses and that alternatively, a larger gradient for a smaller rainout fraction may represent greater amounts of prior rainout upwind of the sampling locations.

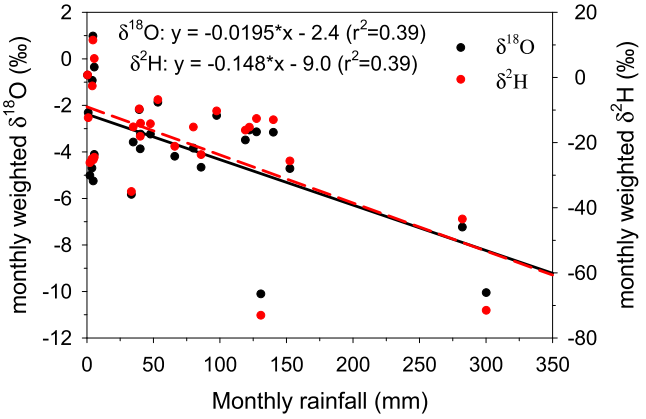

Fig. 5. Significant inverse correlation was observed between rainfall amount and $\delta^{18}O$ and δ^2H ($p < 0.05$). We used rainfall $\delta^{18}O$ and δ^2H data from the FAMU campus site and rain amount data from a nearby weather station (2014–2017) for the graph.

3.2. Stable oxygen and hydrogen isotopes in soil pore waters and natural surface waters

Soil pore water had a much narrower $\delta^{18}O$ range from −4.2 to −2.5‰ (−3.1 ± 0.6‰, n = 9) and δ^2H from −18.3 to −7.0‰ (−14.0 ± 3.2‰, n = 9) (mean ± sd represented as pink star, Fig. 4) than those of the rains. While more depleted $\delta^{18}O$ values were observed in 2015 (−3.9 ± 0.3‰, n = 3) compared to either 2016 (−2.8 ± 0.1‰, n = 3) and 2017 (−2.7 ± 0.2‰, n = 3), there was no significant difference ($p < 0.05$) in δ^2H values during the three years (2015: −15.6 ± 0.5‰, n = 3; 2016: −15.6 ± 2.4‰, n = 3; 2017: −10.8 ± 3.4‰, n = 3). Overall, these $\delta^{18}O$ values were slightly more enriched compared to the weighted mean rain $\delta^{18}O$ value of −5.1‰. With a limestone geology and fast groundwater recharge, the groundwater isotopic signature could be similar to the rainfall isotopic signature, especially when rainfall exceeded ~90 mm/month (Govender et al., 2013).

The mean soil pore water isotope value obtained in this study was similar to those by Katz (2001), which observed a mean WKP groundwater isotope $\delta^{18}O$ and δ^2H valuesof −3.8 ± 0.4‰ (n = 11) and −19.7 ± 2.8‰ (n = 11), respectively, and that of a nearby Wakulla Springs ($\delta^{18}O$ = −3.5‰, δ^2H = −18.4‰). The Wakulla Springs is one of the major springs in Florida that discharges millions of gallons of water per day to the Wakulla River. Katz (2001) further observed that the WKP groundwater $\delta^{18}O$-δ^2H data showed a regression line slope ($\delta^2H = 6.2*\delta^{18}O + 3.9$ ($r^2 = 0.90$, n = 11) which indicated isotope enrichment relative to either the GMWL or the LMWL.

Temporal ambient surface water samples were collected from Pond 55, Pond 12 and Blue Sink from 2014 to 2017. Overall, the range of isotope values was from −2 to +4.2‰ for $\delta^{18}O$ and from −24.3 to +16.4‰ for δ^2H (Table 5). Lower (< 10) or negative d-excess values in the ponds compared to precipitation indicate fractionation effects due

Table 5
Descriptive statistics of ambient natural surface water oxygen and hydrogen isotopes collected in 2014–2017. Numbers enclosed in parentheses denote standard deviations.

Site	Statistic	$\delta^{18}O$ (‰)	$\delta^{2}H$ (‰)	d-excess
all	min	−2.0	−24.3	−28.7
	max	4.2	16.4	9.7
	median	0.9	−1.2	−7.6
	mean	0.9 (1.2)	−0.7 (7.4)	−7.8 (5.2)
	n	175	175	175
Pond 55	min	−2.0	−24.3	−28.7
	max	3.9	12.0	9.7
	median	0.8	−2.0	−8.6
	mean	0.7 (1.3)	−2.3 (8.6)	−7.6 (6.5)
	n	72	72	72
Pond 12	min	−0.5	−15.2	−17.4
	max	4.2	16.4	1.4
	median	1.5	5.1	−10.5
	mean	1.7 (1.3)	4.1 (8.4)	−9.8 (5.2)
	n	34	34	34
Blue Sink	min	−0.7	−13.1	−13.7
	max	2.1	4.1	2.6
	median	0.6	−1.4	−6.9
	mean	0.7 (0.6)	−1.6 (3.6)	−6.9 (3.2)
	n	69	69	69

Table 6
$\delta^{18}O$-$\delta^{2}H$ regression lines of selected ponds and sinks within the Apalachicola National Forest.

Site	$\delta^{18}O$-$\delta^{2}H$ regression line	r^2	n
Pond 55	$\delta^{2}H = 5.1*\delta^{18}O - 5.7$	0.63	72
Blue Sink	$\delta^{2}H = 4.5*\delta^{18}O - 4.6$	0.58	69
Pond 12	$\delta^{2}H = 5.6*\delta^{18}O - 5.6$	0.77	34

to evaporation as observed by other studies (e.g., Reckerth et al., 2017). Seasonality in isotopic signatures were not observed in either Pond 55 or Blue Sink ($p < 0.05$). Observed slopes of the $\delta^{18}O$-$\delta^{2}H$ regression line between 4.5 and 5.6 indicated that overall the natural surface waters in the area were significantly evaporated (Table 6).

Rain and groundwater are potential sources of natural surface waters within the ANF. Based on water table changes and measurements of pH and alkalinity, it was speculated by Milla et al. (in Odezulu, 2011) that the water of a nearby ephemeral ANF Pond 1 was mostly rain-derived while that of Blue Sink was a mixture of rainwater and groundwater. Based on our isotopic data (Table 6), the measured LMWL and the Pond 55 $\delta^{18}O$-$\delta^{2}H$ regression line intersect at the point of −5.7‰ ($\delta^{18}O$) and −34.7‰ ($\delta^{2}H$). These values are similar to that of the mean weighted rain isotope values of −5.1‰ ($\delta^{18}O$) and −30.2‰ ($\delta^{2}H$). Our isotopic results confirm that the source of the surface water in Pond 55 was indeed mostly from rain. On the other hand, the LMWL and the Blue Sink $\delta^{18}O$-$\delta^{2}H$ regression line intersected at the point of −4.3‰ ($\delta^{18}O$) and −24.0‰ ($\delta^{2}H$), which were more enriched than the mean rainwater isotope values, indicating another possible water source other than the local rains.

3.3. Sensitivity of using isotopes as tracers to quantify hydrology of the wetlands

This study shows that the difference in isotopic signature between the rain and the surface water was significant and could be used to trace the contribution of a rain to the surface water of a wetland, especially during tropical storms and hurricanes (Tables 1 and 5). For example, the rain carried by the tropical storm Colin had mean $\delta^{18}O$ and $\delta^{2}H$ of −12.5‰ and −92.9‰, respectively. The surface water of Pond 55 had mean $\delta^{18}O$ and $\delta^{2}H$ of 0.7‰ (min. −2 and max. 3.9) and –2.3‰ (min. −24.3 and max. 12.0), respectively, during the study period. The minimum and maximum combined $\delta^{18}O$ and $\delta^{2}H$ isotopic differences on a $\delta^{18}O$ and $\delta^{2}H$ plot between tropical storm Colin and the Pond 55 surface water were 69.4‰ and 106.2‰, respectively. The combined error of the $\delta^{18}O$ and $\delta^{2}H$ plot was about 2‰. The uncertainty of using the isotopic signals to trace the contribution of the tropical storm Colin rain to the surface water of Pond 55 would be in a range between 1.9 and 2.9% of the total surface water volume. In other words, the contribution of the tropical storm Colin to the surface water of Pond 55 can be sensitively quantified using the isotopic signals with the resolution of 1.9–2.9% of the total surface water volume. Similar analysis for the Blue Sink indicated the resolution of rain water contribution from tropical storm Colin to be in the range between 2.0 and 2.5% of the total surface water volume. In case of the hurricane Hermine event, the resolution of rain water contribution to Pond 55 would be in a range between 2.3 and 4.1% of the total surface water volume and that of the Blue Sink would be between 2.6 and 3.3% of the total surface water volume. The surface water volumes of those wetlands are relatively small, in which the increase of the surface water during a storm could easily exceed > 10% of the total water volume. The rainfall contribution to the Pond 55 during the Category 1 hurricane Hermine was 38 ± 3% according to the isotopic signals.

While tropical storms and hurricanes like Colin and Hermine provide us with most desirable opportunities to trace the hydrology of those wetlands, other rains also may provide good opportunities as well. We used the most and least depleted rains other than tropical storms and hurricanes to calculate the uncertainty (resolution) of rain water contribution to the surface water of those wetlands. The results showed that in case of Pond 55, the resolution ranged from 4.6 to 30.0% of the total surface water volume and in case of the Blue Sink it ranged from 5.7 to 11.3% of the total surface water volume. In the case of tropical storm Cindy, the resolution of rain contribution to Pond 55 and Blue Sink total surface water volumes ranged 5.2–65.2% and 6.6–15.5%, respectively. The much higher maximum uncertainty (65.2%) could still occur especially when preceded by other tropical storms or hurricanes. These results show that not all rain events were suitable for the tracer approach but many heavier rain events were.

The estimated contribution of the rain water to the surface water of the wetlands by the isotopic method are all in relative terms, i.e., % of the total water volume and applicable to only a specific rain event. We can convert those % increase in water volumes to the absolute water storage of the pond, however, by the following strategy: First, we need to construct the water depth vs. surface area relationship by topographic contour plot and surface water area vs. water depth (to a reference point) measurements. Then we can convert the surface water area vs water depth relationship to a delta water volume increase vs water depth (to the reference level) increase relationship. With this delta water volume increase vs water depth (to the reference level) increase information, we can identify the corresponding % water volume increase by the isotopic method during a runoff event and calculate the absolute water volume of the pond at that water depth (to the reference level). We then have a very convenient means to know the absolute water storage of the pond at any given time by just knowing the water depth (to the reference level) of a pond at that time. Monitoring changes in surface water depth (to the reference level) then becomes a convenient way to quantify hydrologic parameters of the drainage area around the wetland such as runoff/precipitation ratio, charge/discharge rates of the wetland, evapotranspiration rate of the drainage area and evaporation rate of the surface water.

3.4. Evaporation extent of isolated forested wetlands

Isotopic enrichment of a water body relative to its potential sources is an indication of evaporation. Assuming isotopic equilibrium between the liquid and vapor phases, the degree of primary evaporation of the water body at a given temperature and humidity can be calculated using the Craig-Gordon (C-G) model (Gonfiantini, 1986; Majoube,

1971; Clark and Fritz, 1997; Murad and Krishnamurthy, 2008).

$$\Delta(O/H) = \varepsilon_{total\_(O/H)} * \ln(f_{rw}) = (\varepsilon_{w-v} + \varepsilon_{v-bl}) * \ln(f_{rw}) \quad (2)$$

$$\Delta = \delta_o - \delta_i = (\varepsilon_{w-v} + \varepsilon_{v-bl}) * \ln(f_{rw}) \quad (3)$$

$$f_{rw} = e^{(\Delta/\varepsilon total)} \quad (4)$$

$$f_{ev} = 1 - f_{rw} \quad (5)$$

where $\Delta(O/H)$ is the difference in $\delta^{18}O$ or δ^2H of the original unevaporated source water (subscript "o") and temporal water body (subscript "i"), f_{rw} and f_{ev} are the remaining and evaporated water fractions, respectively. The isotope signatures of the original unevaporated water source can be calculated from the intersection of the LMWL and LEL (assuming a single source of water) while evaporative water loss can be calculated from Eqns. (2)–(9) (also see below). The term $\varepsilon_{total\_(O/H)}$ represents the equilibrium and kinetic fractionations of the O and H isotopes at the water–vapor (w-v) and evaporation [i.e., vapor-boundary layer (v-bl)] interfaces, respectively, and are calculated using the following equations (Gonfiantini, 1986; Majoube, 1971; Araguás-Araguás et al., 2000):

For ^{18}O:
$$\varepsilon_{w-v}(‰) = (1.137 \times 10^6/T^2) + (0.4156 \times 10^3/T) + 2.0667 \quad (6)$$

$$\varepsilon_{v-bl}(‰) = (h - 1) \times 14.2 \quad (7)$$

For ^{H}:
$$\varepsilon_{w-v}(‰) = (-24.844 \times 10^6/T^2) + (76.248 \times 10^3/T) - 52.612 \quad (8)$$

$$\varepsilon_{v-bl}(‰) = (h - 1) \times 12.5 \quad (9)$$

where temperature (T) and humidity (h) are expressed in Kelvin units and a fraction, respectively. Average sampling day temperature and humidity values taken from online meteorological data were used in the calculations.

Benettin et al. (2018) argued that not all $\delta^{18}O$-δ^2H-regression lines from soil pore waters and xylem waters can be called LELs due to possible multiple sources of waters. For Ponds 55 and 12 and other ponds that are derived from a single source of water, we can use the above equations to calculate their possible evaporative losses. Isotope data along the Pond 55 LEL represented calculated evaporative losses that ranged from 20 to 48% with a mean of 35.3 ± 7.3% (n = 72, Fig. 6) during the study period. On the other hand, mean evaporative loss at Pond 12 was 46.9 ± 7.3% (n = 34, Fig. 6) during the study period. Pond 12 has much shallower profile and larger surface/depth ratio than Pond 55, which explains the more significant evaporation observed in the surface water. According to previous studies, the evaporative enrichment is a dominant factor in the isotope balance of closed or lentic hydrological systems such as lakes and wetlands (e.g., Krabbenhoft et al., 1990; Meyers et al., 1993; Saxena, 1996; Gremillion and Wanielista, 2000; Marimuthu et al., 2005). With the isotope repeated measurement error of 0.3‰ and 2‰ for $\delta^{18}O$ and δ^2H, respectively, uncertainties in % evaporative loss measurements can be calculated from isotope gradient, % evaporative loss and the repeated measurement error: % evaporative loss measurement uncertainty = [% evaporation loss × 0.3‰ (for $\delta^{18}O$ or 2‰ for δ^2H)]/isotope gradient. Low calculated % evaporative loss measurement with uncertainties of 1.8 ± 0.2% (for $\delta^{18}O$-based) and 2.0 ± 0.2% (δ^2H-based) gave good confidence to the estimated evaporative losses of the two ponds, as long as the latter values are significantly above the measurement uncertainties.

For Pond 55, the passage of hurricane Hermine followed by a prolonged dry period (85 days) gave us an opportunity to estimate the extent of evaporation during the dry period. With the Pond 55 LEL being $\delta^2H = 5.2*\delta^{18}O - 13.7$ ($r^2 = 0.98$, n = 8), the intersection of this LEL with the LMWL is at −9.2‰ and −61.3‰ for $\delta^{18}O$ and δ^2H, respectively. We sampled the water between the 15th and 85th days after the hurricane. Evaporative loss during the 70-day dry period caused the $\delta^{18}O$ and δ^2H of Pond 55 surface water to be enriched by 3.7‰ and 16.2‰, respectively (Fig. 7). The evaporation loss was calculated to be 20.5 ± 3.5% of the original surface water volume. The isotope data for Pond 12, on the other hand, encompassed the 46 dry days between

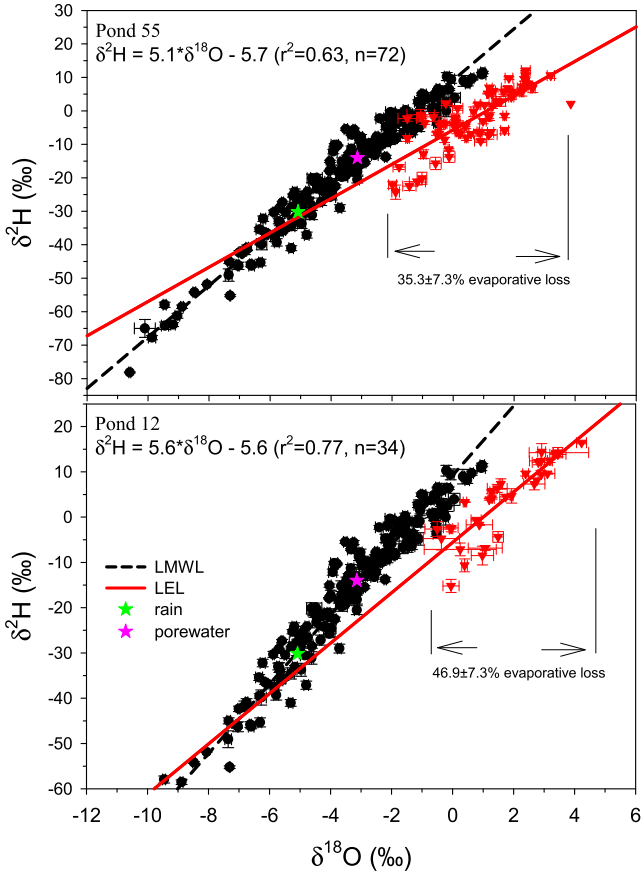

Fig. 6. Evaporative losses in single water source Pond 55 and Pond 12 as calculated using the C-G model (Eqs. (2)–(9)). Mean sampling day temperature and humidity values were used in the calculation. The y-axis for both sites depicts different scales. The green star represents the mean weighted isotopic rain signature of all data ($\delta^{18}O$ = −5.1‰, δ^2H = −30.2‰). The pink star represents the mean pore water isotope signature ($\delta^{18}O$ = −3.1 ± 0.6‰, δ^2H = −14.0 ± 3.2‰, n = 9).

water samplings which showed $\delta^{18}O$ and δ^2H enrichments to be 1.5‰ and 10.8‰, respectively (Fig. 7). The evaporation loss over the 46-day dry period was calculated to be 11.3 ± 0.4% of the original surface water.

Unlike the cases of the rainwater-fed Pond 55 and 12, Blue Sink had the mixed contribution of rain and groundwater, whose isotopic signature was unknown. The evaporation of the Blue Sink, therefore, cannot be deduced similarly from the LEL. However, the Blue Sink LEL during this extended dry period ($\delta^2H = 5.9*\delta^{18}O - 7.5$, $r^2 = 0.93$, n = 8) intersected the LMWL at $\delta^{18}O$ = −9.3‰ and δ^2H = −62.2‰, very similar to that of the Pond 55 ($\delta^{18}O$ = −9.2‰ and δ^2H = −61.3‰) and close to the signals of the hurricane Hermine rainfall ($\delta^{18}O$ = −11.1 ± 3.1‰ and δ^2H = −80.4 ± 25.9‰, n = 7). We, therefore, suspect that the rainwater of hurricane Hermine probably contributed to the majority of the surface water both in Pond 55 and Blue Sink right after the event. With that assumption, we estimated the evaporation loss of the Blue Sink during the 70 day dry period to be 13.1 ± 0.2%. Blue Sink ^{18}O and ^2H enrichments reached 1.9‰ and 12.0‰, respectively (Fig. 7).

In the laboratory, the 14-day beaker evaporation experiment using Pond 55 waters yielded a total accumulated evaporative loss of 57.5 ± 1.3% with an accompanying +5.0‰ and +27.6‰ enrichment of the ^{18}O and ^2H isotopes, respectively. We observed a significant direct correlation between the measured laboratory beaker evaporation losses and those calculated using the C-G model (Fig. 8, $p < 0.05$). Other pan evaporation rate studies (e.g., Gibson et al., 1999; van den

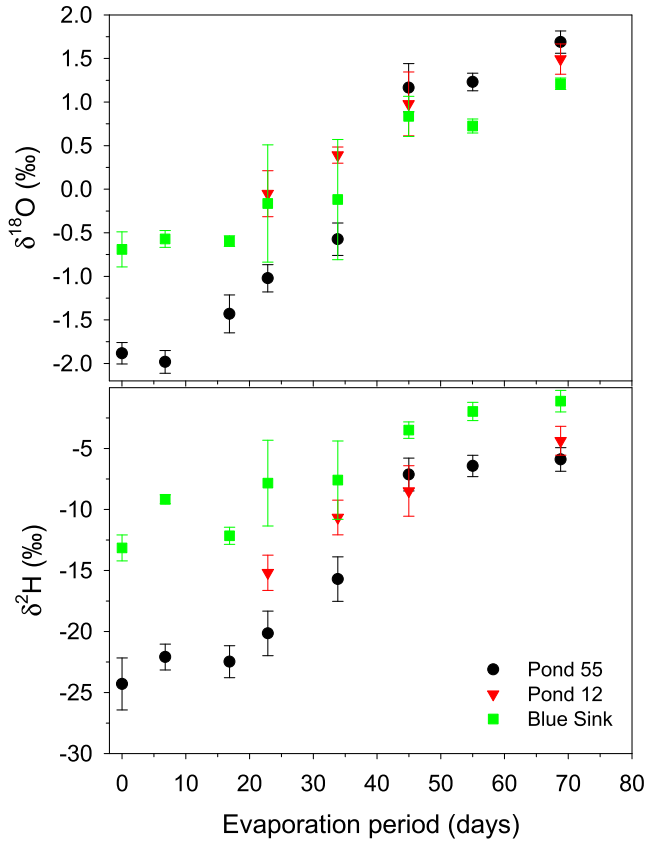

Fig. 7. $\delta^{18}O$ and $\delta^{2}H$ of water samples collected at Pond 55, Pond 12 and Blue Sink after the passage of a hurricane followed by an evaporation period of up to 70 days. ^{18}O and ^{2}H enrichments as high 3.7‰ and 16.2‰ were observed at end of the dry period, respectively.

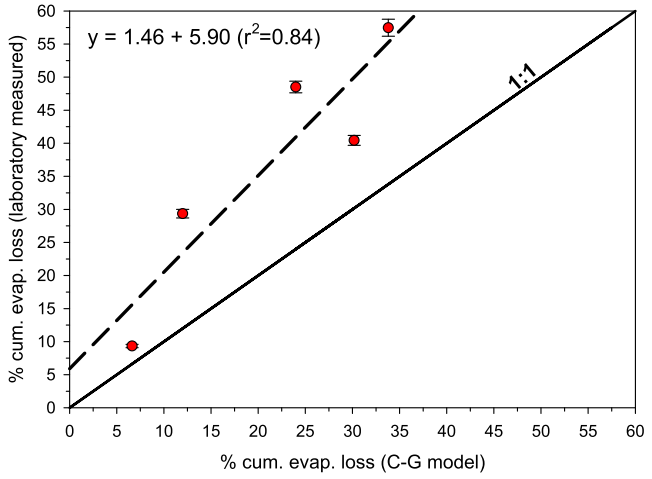

Fig. 8. Measured evaporative loss versus calculated evaporative loss. There is a significant direct correlation between the 2 parameters ($p < 0.05$).

Akker et al., 2011) have reported results with high direct regression coefficients ($r^2 > 0.9$) and with mostly 1:1 correlations between their measured and theoretical values. This is in contrast to our study in which laboratory measured values were much higher than those that were calculated (Fig. 8). As other studies had pointed out, small drying pans (< 1 L) are oversensitive to atmospheric conditions and provide information that is less hydrologically useful (e.g., Welhan and Fritz, 1977; Gonfiantini, 1986; Gibson et al., 1999). However, even with the small drying pan size, the 2-week laboratory experiment still demonstrated a Pond 55 evaporation line of $\delta^{2}H = 5.3*\delta^{18}O - 6.2$ ($r^2 = 0.99$, n = 5) that was similar to the measured LEL ($\delta^{2}H = 5.1*\delta^{18}O - 5.7$, $r^2 = 0.63$, n = 72; Table 6). Furthermore, the closed bottom PVC set up installed upslope of Pond 55 also showed a similar LEL ($\delta^{2}H = 5.5*\delta^{18}O - 4.8$, $r^2 = 0.80$, n = 57). Gibson and Reid (2014) also reported evaporation pan $\delta^{18}O$ and $\delta^{2}H$ values were similar to the lake isotope values. Pond 12, another isolated wetland in our study area, also showed similar LELs between its natural surface waters ($\delta^{2}H = 5.6*\delta^{18}O - 5.6$, $r^2 = 0.77$, n = 34; Table 6) and PVC counterpart ($\delta^{2}H = 5.4*\delta^{18}O - 4.3$, $r^2 = 0.90$, n = 16). The LEL comparison of waters from Pond 55, and the PVC and beaker experiments suggest that in a hydrological system in which precipitation and evaporation serve as the dominant inflow and outflow conduits such as isolated wetlands, the isotopic signature of water can serve as a powerful tracer for studying the water balance due to evaporation. We believe that the results we had obtained from this study can be applied to the similar isolated wetlands in the Apalachicola National Forest and other humid subtropical regions. While not a subject of this research, the use of the water isotope tracer techniques could also be applied to study the hydrological processes of other isolated palustrine systems such as those dominated by and have more than 50% areal coverage of deciduous trees and shrubs (National Wetlands Inventory, accessed 27-Oct-2019). This study confirms the sensitivity of the approach and gives us a valuable guidance to our subsequent study of the hydrology in those isolated wetlands in the region.

4. Conclusion

This study has documented the stable isotope signals of the rain, the soil pore water and the surface water of the study area. The results show the sensitivity and resolution of using the stable isotopic signals to quantify the hydrology of those wetlands. The measured local meteoric water line follows closely the global meteoric water line, indicating minimal evaporation during rainfall. We observed no significant correlations between isotopic signatures with either temperature or relative humidity. There was lacking seasonality in the isotopic signatures except during the hurricane season when hurricanes and tropical storms contribute much depleted isotopic signals. We did observe a significant inverse correlation between isotopes and rainfall amount. We were able to show that the ephemeral ponds Pond 55 and Pond 12 were mainly derived from rain water and that the Blue Sink has water source other than rain water. This study shows that the $\delta^{18}O$ and $\delta^{2}H$ of rains, especially heavier rains were significantly depleted in comparison to those of the surface water of the wetlands. Those significant differences in stable isotopic signals can be used to trace the contribution of rain water to the surface water, the sources of surface water and the extent of surface evaporation of those wetlands. The stable isotope tracers can be a powerful and much simpler tool in the study of hydrology of those scattered isolated wetlands in the southeastern US in comparison to the traditional hydrologic monitoring methods.

Declaration of Competing Interest

The authors declare that they have no known competing financial interests or personal relationships that could have appeared to influence the work reported in this paper.

Acknowledgements

This study was funded by the USDA Forest Service (USA) under Grant agreement no. 15-CA-11330140-026 awarded to Y.-P. Hsieh. We thank Djanan Nemours, Isaac Ogunrinde, Gabriel Omoniyi, Vanessa Baretto, Lucy Ngatia, Samuel Olaborode and Gbemisola Akinbi for their assistance in the field work of this research. We thank the editor and the reviewers for their insightful comments.

References

Allen, S.T., Keim, R.F., Barnard, H.R., McDonnell, J.J., Brooks, J.R., 2017. The role of stable isotopes in understanding rainfall interception processes: a review. WIREs Water 4, e1187. https://doi.org/10.1002/wat2.1187.

Araguás-Araguás, L., Froehlich, K., Rozanski, K., 2000. Deuterium and oxygen-18 isotope composition of precipitation and atmospheric moisture. Hydrol. Process. 14, 1341–1355.

Baczynski, A.A., McInerney, F.A., Wing, S.L., Kraus, M.J., Bloch, J.I., Secord, R., 2017. Constraining paleohydrologic change during the Paleocene-Eocene Thermal Maximum in the continental interior of North America. Palaeogeogr. Palaeoclimatol. Palaeoecol. 465, 237–246.

Baer, D.S., Paul, J.B., Gupta, M., O'Keefe, A., 2002. Sensitive absorption measurements in the near infrared region using off-axis integrated-cavity output spectroscopy. Appl. Phys. B 75, 261–265.

Bauder, E.T., 2005. The effects of an unpredictable precipitation regime on vernal pool hydrology. Freshwater Biol. 50, 2129–2135.

Benettin, P., Volkmann, T.H.M., von Freyberg, J., Frentress, J., Penna, D., Dawson, T.E., Kirchner, J.W., 2018. Effects of climatic seasonality on the isotopic composition of evaporating soil waters. Hydrol. Earth Syst. Sci. 22, 2881–2890.

Berman, E.S., Levin, N.E., Landais, A., Li, S., Owano, T., 2013. Measurement of $\delta^{18}O$, $\delta^{17}O$, and $\delta^{17}O$-excess in water by off-axis integrated cavity output spectroscopy and isotope ratio mass spectrometry. Anal. Chem. 85, 10392–10398.

Breitenbach, S.F.M., Adkins, J.F., Meyer, H., Marwan, N., Kumar, K.K., Haug, G.H., 2010. Strong influence of water vapor source dynamics on stable isotopes in precipitation observed in Southern Meghalaya, NE India. Earth Planet. Sci. Lett. 292, 212–220.

Brooks, R.T., 2009. Potential impacts of global climate change on the hydrology and ecology of ephemeral freshwater systems of the forests of the northeastern United States. Clim. Change 95, 469–483.

Chandler, H.C., Rypel, A.L., Jiao, Y., Haas, C.A., Gorman, T.A., 2016. Hindcasting Historical Breeding Conditions for an Endangered Salamander in Ephemeral Wetlands of the Southeastern USA: Implications of Climate Change. PLoS ONE 11, e0150169. https://doi.org/10.1371/journal.pone.0150169.

Chandler, H.C., McLaughlin, D.L., Gorman, T.A., McGuire, K.J., Feaga, J.B., Haas, C.A., 2017. Drying Rates of Ephemeral Wetlands: Implications for Breeding Amphibians. Wetlands 37, 545–557.

Clark, I.D., Fritz, P., 1997. Environmental Isotopes in Hydrogeology. CRC Press, Boca Raton.

Coplen, T.B., Herczeg, A.L., Barnes, C., 2000. Isotope engineering-using stable isotopes of water molecule to solve practical problems. In: Cook, P., Herczeg, A.L. (Eds.), Environmental tracers in catchment hydrology. Kluwer Academic Publishers, Norwell, pp. 79–110.

Craig, H., 1961. Isotopic variations in meteoric waters. Science 133, 1702–1708.

Dansgaard, W., 1964. Stable isotopes in precipitation. Tellus 16, 436–468.

Davis, H., 1996. Hydrogeologic Investigation and Simulation of Ground-Water Flow in the Upper Floridan Aquifer of North-Central Florida and Southwestern Georgia and Delineation of Contributing Areas for Selected City of Tallahassee, Florida, Water-Supply Wells. U.S. Geological Survey Water-Resources Investigations Report 95-4296. U.S. Geological Survey Earth Science Information Center, Denver, CO.

Dogramaci, S., Skrzypek, G., Dodson, W., Grierso, P.F., 2012. Stable isotope and hydrochemical evolution of groundwater in the semi-arid Hamersley Basin of subtropical northwest Australia. J. Hydrol. 475, 281–293.

Fricke, H.C., O'Neil Jr., J., 1999. The correlation between $^{18}O/^{16}O$ ratios of meteoric water and surface temperature: its use in investigating terrestrial climate change over geologic time. Earth Planet. Sci. Lett. 170, 181–196.

Gammons, C.H., Poulson, S.R., Pellicori, D.A., Reed, P.J., Roesler, A.J., Petrescu, E.M., 2006. The hydrogen and oxygen isotopic composition of precipitation, evaporated mine water, and river water in Montana, USA. J. Hydrol. 328, 319–330.

Gat, J.R., 1996. Oxygen and hydrogen isotopes in the hydrologic cycle. Annu. Rev. Earth Planet. Sci. 24, 225–262.

Gautam, M.K., Lee, K.-S., Bong, Y.-S., Song, B.-Y., Ryu, J.-S., 2017. Oxygen and hydrogen isotopic characterization of rainfall and throughfall in four South Korean cool temperate forests. Hydrol. Sci. J. 62, 2025–2034.

Gedzelman, S.D., Lawrence, J.R., 1982. The isotopic composition of cyclonic precipitation. J. Appl. Meteorol. 21, 1385–1404.

Gedzelman, S.D., Lawrence, J.R., 1990. The isotopic composition of precipitation from two extratropical cyclones. Mon. Weather Rev. 118, 495–509.

Gibson, J.J., Edwards, T.W.D., Prows, T.D., 1999. Pan-derived isotopic composition of atmospheric water vapour and its variability in northern Canada. J. Hydrol. 217, 55–74.

Gibson, J.J., Birks, S.J., Edwards, T.W.D., 2008. Global prediction of δ_A and δ^2H-$\delta^{18}O$ evaporation slopes for lakes and soil water accounting for seasonality. Global Biogeochem. Cy. 22, GB2031. https://doi.org/10.1029/2007GB002997.

Gibson, J.J., Reid, R., 2014. Water balance along a chain of tundra lakes: A 20-year isotopic perspective. J. Hydrol. 519, 2148–2164.

Gonfiantini, R., 1986. Environmental isotopes in lake studies. In: Fritz, B.P., Fontes, J.C. (Eds.), Handbook of Environmental Isotope Geochemistry: Vol 2, The Terrestrial Environment. Elsevier, Amsterdam, The Netherlands, pp. 113–168.

Good, S.P., Mallia, D.V., Lin, J.C., Bowen, G.J., 2014. Stable isotope analysis of precipitation samples obtained via crowdsourcing reveals the spatiotemporal evolution of Superstorm Sandy. PLoS ONE 9, e91117. https://doi.org/10.1371/journal.pone.0091117.

Govender, Y., Cuevas, E., Sternberg, L.D.S., Jury, M.R., 2013. Temporal Variation in Stable Isotopic Composition of Rainfall and Groundwater in a Tropical Dry Forest in the Northeastern Caribbean. Earth Interact. 17 (27), 1–20. https://doi.org/10.1175/2013EI000534.1.

Gremillion, P., Wanielista, M., 2000. Effects of evaporative enrichment on the stable isotope hydrology of a central Florida (USA) river. Hydrol. Process. 14, 1465–1484.

Greenberg, C.H., Goodrick, S., Austin, J.D., Parresol, B.R., 2015. Hydroregime Prediction Models for Ephemeral Groundwater-Driven Sinkhole Wetlands: a Planning Tool for Climate Change and Amphibian Conservation. Wetlands 35, 899–911.

Hartley, P.E., 1981. Deuterium/hydrogen ratios in Australian rainfall. J. Hydrol. 50, 217–229.

Harvey, F.E., 2001. Use of NADP archive samples to determine the isotope composition of precipitation: characterizing the meteoric input function for use in ground water studies. Groundwater 39, 380–390.

Hayashi, M., Rosenberry, D.O., 2002. Effects of ground water exchange on the hydrology and ecology of surface water. Groundwater 40, 309–316.

Hendry Jr., C.W., Sproul, C.R., 1966. Geology and ground water resources of Leon County, Florida. Florida Geol. Survey Bull. 47, 178 p.

Johnson, E.E., Gjerstad, D., 2006. Restoring the overstory of longleaf pine ecosystems. In: Jose, S., Jokela, E.J., Miller, D.L. (Eds.), The Longleaf Pine Ecosystem: Ecology, Silviculture, and Restoration. Springer, New York, pp. 271–295.

Katz, B.G., 2001. A Multracer Approach for Assessing the Susceptibility of Ground-Water Contamination in the Woodville Karst Plain, Northern Florida. In U.S. Geological Survey Karst Interest Group Proceedings, Water-Resources Investigations Report 01-4011, E.L. Kuniansky (Ed). 167-176.

Katz, B.G., Bullen, T.D., 1996. The combined use of $^{87}Sr/^{86}Sr$ and carbon and water isotopes to study the hydrochemical interaction between groundwater and lakewater in mantled karst. Geochim. Cosmochim. Acta 60, 5075–5087.

Kincaid, T., C.L. Werner, 2008. Karst Hydrogeology of the Woodville Karst Plain Florida. In: Sinkholes and the Engineering and Environmental Impacts of Karst, Edition: Geotechnical Special Publication No. 33; Field Trip Guidebook, Publisher: American Society of Civil Engineers.

Koch, P.L., Zachos, J.C., Dettman, D.L., 1995. Stable-isotope stratigraphy and paleoclimatology of the Paleogene Bighorn Basin (Wyoming, USA). Palaeogeogr Palaeoclimatol Palaeoecol. 115, 61–89.

Krabbenhoft, D.P., Bowser, C.J., Anderson, M.P., Valley, J.W., 1990. Estimating groundwater exchange with lakes. The stable isotope mass balance method. Water Resour. Res. 26, 2445–2453.

Lachniet, M.S., Patterson, W.P., 2009. Oxygen isotope values of precipitation and surface waters in northern Central America (Belize and Guatemala) are dominated by temperature and amount effects. Earth Planet. Sci. Lett. 284, 435–446.

Lambert, W.J., Aharon, P., 2010. Oxygen and hydrogen isotopes of rainfall and dripwater at DeSoto Caverns (Alabama, USA): Key to understanding past variability of moisture transport from the Gulf of Mexico. Geochim. Cosmochim. Acta 74, 846–861.

Lane, C.S., Hildebrandt, B., Kennedy, L.M., LeBlanc, A., Liu, K.B., Wagner, A.J., Hawkes, A.D., 2017. Verification of tropical cyclone deposits with oxygen isotope analyses of coeval ostracod valves. J. Paleolimnol. 57, 245–255.

Lawrence, J.R., 1998. Isotopic spikes from tropical cyclones in surface waters: Opportunities in hydrology and paleoclimatology. Chem. Geol. 144, 153–160.

Lawrence, J.R., Gedzelman, S.D., 1996. Low stable isotope ratios of tropical cyclone rains. Geophys. Res. Lett. 23, 527–530.

Lawrence, J.R., Gedzelman, S.D., Zhang, X., Arnold, R., 1998. Stable isotope ratios of rain and vapor in 1995 hurricanes. J. Geophys. Res. 103, 11381–11400.

Lawrence, J.R., Gedzelman, S.D., Gamache, J., Black, M., 2002. Stable Isotope Ratios: Hurricane Olivia. J. Atmos. Chem. 41, 67–82.

Lis, G., Wassenaar, L.I., Hendry, M.J., 2008. High-precision laser spectroscopy D/H and $^{18}O/^{16}O$ measurements of microliter natural water samples. Anal. Chem. 80, 287–293.

Majoube, M., 1971. Fraction in O-18 between ice and water vapor. J. Chim. Phys. 68, 625–636.

Marimuthu, S., Reynolds, D.A., Le Gal La Salle, C., 2005. A field study of hydraulic, geochemical and stable isotope relationships in a coastal wetlands system. J. Hydrol. 315, 93–116.

Means, R., 2008. Management strategies for Florida's ephemeral ponds and pond-breeding amphibians, Final Report. Coastal Plains Institute, Inc., Tallahassee, FL, 109p. https://www.coastalplains.org/research/cpi-publications/#Books.

Means, R.C., R.P.M. Means, M. Beshel, R. Mendyk, P. Hill, M. Hoffman, S. Reichling, and B. Summerford, 2017. A conservation strategy for the imperiled western striped newt in the Apalachicola National Forest, FL. Seventh Annual Report. Coastal Plains Institute, Inc., Tallahassee, FL, 40p. (https://www.coastalplains.org/research/cpi-publications/#Books).

Meyers, J.B., Swart, P.K., Meyers, J.L., 1993. Geochemical evidence for groundwater behavior in an unconfined aquifer, south Florida. J. Hydrol. 148, 249–272.

Midwood, A.J., Boutton, T.W., Archer, S.R., Watts, S.E., 1998. Water use by woody plants on contrasting soils in a savanna parkland: assessment with δ^2H and $\delta^{18}O$. Plant Soil 205, 13–24.

Murad, A.A., Krishnamurthy, R.V., 2008. Factors controlling stable oxygen, hydrogen and carbon isotopes ratios in regional groundwater of the eastern United Arab Emirates. Hydrol. Process. 22, 1922–1931.

National Wetlands Inventory, 2019. US Fish and Wildlife Service (https://www.fws.gov/wetlands/data/mapper.html).

Odezulu, C.I., 2011. Stable hydrogen and oxygen isotopic variations in natural waters in North Florida: implications for hydrological and paleoclimatic studies. M.S. Thesis, Florida State University, Tallahassee, FL, 59 p.

Onac, B.P., Pace-Graczyk, K., Atudirei, V., 2008. Stable isotope study of precipitation and cave drip water in Florida (USA): implications for speleothem-based paleoclimate studies. Isotopes Environ. Health Stud. 44, 149–161.

Oswalt, C.M., J.A. Cooper, D.G. Brockway, H.W. Brooks, J.L. Walker, K.F. Connor, S.N. Oswalt, and R.C. Conner, 2012. History and Current Condition of Longleaf Pine in the

Southern United States. USDA Forest Service Southern Research Station General Technical Report SRS–166, Southern Research Station, Asheville, NC 28804. 60 p.
Otte, I., Detsch, F., Gütlein, A., Scholl, M., Kiese, R., Appelhans, T., Nauss, T., 2017. Seasonality of stable isotope composition of atmospheric water input at the southern slopes of Mt. Kilimanjaro, Tanzania. Hydrol. Process. 31, 3932–3947.
Peel, M.C., Finlayson, B.L., McMahon, T.A., 2007. Updated World Map of the Köppen-Geiger Climate Classification. Hydrol. Earth Syst. Sci. 11, 1633–1644.
Penna, D., Stenni, B., Šanda, M., Wrede, S., Bogaard, T.A., Gobbi, A., Borga, M., Fischer, B.M.C., Bonazza, M., Chárová, Z., 2010. On the reproducibility and repeatability of laser absorption spectroscopy measurements for δ^2H and $\delta^{18}O$ isotopic analysis. Hydrol. Earth Syst. Sci. 14, 1551–1566.
Permana, D.S., Thompson, L.G., Setyadi, G., 2016. Tropical West Pacific moisture dynamics and climate controls on rainfall isotopic ratios in southern Papua, Indonesia. J. Geophys. Res. Atmos. 121, 2222–2245.
Reckerth, A., Stichler, W., Schmidt, A., Stumpp, C., 2017. Long-term data set analysis of stable isotopic composition in German rivers. J. Hydrol. 552, 718–731.
Rozanski, K., Araguás-Araguás, L., Gonfiantini, R., 1992. Relation between long-term trends of Oxygen-18 isotope composition of precipitation and climate. Science 258, 981–985.
Roznik, E.A., Johnson, S.A., Greenberg, C.H., 2009. Terrestrial movements and habitat use of gopher frogs in longleaf pine forests: a comparative study of juveniles and adults. Forest Ecol. Manag. 259, 187–194.
Rupert, F.R., 1988. The geology of Wakulla Springs. Florida Geological Survey Open-File Report 22, 18 p.
Saxena, R.K., 1996. Estimation of lake evaporation from a shallow lake in central Sweden by Oxygen-18. Hydrol. Process. 10, 1273–1281.
Seal, R.R., Shanks, W.C., 1998. Oxygen and hydrogen isotope systematics of Lake Baikal, Siberia: Implications for paleoclimate studies. Limnol. Oceanogr. 43, 1251–1261.
Sjostrom, D.J., Welker, J.M., 2009. The influence of air mass source on the seasonal isotopic composition of precipitation, eastern USA. J. Geochem. Explor. 102, 103–112.
Soil Survey of Leon County, Florida, 1981. USDA Soil Conservation Service and Forest Service, 162 p.
Sturm, P., Knohl, A., 2010. Water vapor δ^2H and $\delta^{18}O$ measurements using off-axis integrated cavity output spectroscopy. Atmos. Meas. Tech. 3, 67–77.
Tiner, R.W., 2003. Geographically isolated wetlands of the United States. Wetlands 23, 494–516.
van den Akker, J., Simmons, C.T., Hutson, J.L., 2011. Use of stable isotopes deuterium and oxygen-18 to derive evaporation from flood irrigation on the basis of pan evaporation techniques. J. Irrig. Drain Eng. 137, 765–778.
Vieten, R., S. Warken, A. Winter, A. Schroder-Ritzrau, D. Scholz, and C. Spotl, 2018. Hurricane Impact on Seepage Water in Larga Cave, Puerto Rico. J. Geophys. Res. Biogeosci. 123, 879–888.
Wang, S., Zhang, M., Hughes, C.E., Crawford, J., Wang, G., Chen, F., Du, M., Qiu, X., Zhou, S., 2018. Meteoric water lines in arid Central Asia using event-based and monthly data. J. Hydrol. 562, 435–445.
Winter, T.C., Rosenberry, D.O., 1998. Hydrology of prairie pothole wetlands during drought and deluge: A 17-year study of the cottonwood lake wetland complex in North Dakota in the perspective of longer term measured and proxy hydrological records. Clim. Change 40, 189–209.
Welhan, J.A., Fritz, P., 1977. Evaporation pan isotopic behaviour as an index of isotopic evaporation conditions. Geochim. Cosmochim. Acta 41, 682–686.
Welker, J.M., 2000. Isotopic ($\delta^{18}O$) characteristics of weekly precipitation collected across the USA: an initial analysis with application to water source studies. Hydrol. Process. 14, 1449–1464.
Xu, X., Guan, H., Deng, Z., 2014. Isotopic composition of throughfall in pine plantation and native eucalyptus forest in South Australia. J. Hydrol. 514, 150–157.
Zedler, P.H., 2003. Vernal pools and the concept of “isolated wetlands”. Wetlands 23, 597–607.
Zhu, J., Sun, G., Li, W., Zhang, Y., Miao, G., Noormets, A., McNulty, S.G., King, J.S., Kumar, M., Wang, X., 2017. Modeling the potential impacts of climate change on the water table level of selected forested wetlands in the southeastern United States. Hydrol. Earth Syst. Sci. 21, 6289–6305.